Integrated Controls–Structures Design Methodology for Flexible Spacecraft

P. G. Maghami, S. M. Joshi, D. B. Price

Reprinted from

Journal of Spacecraft and Rockets

Volume 32, Number 5, Pages 839–844

AIAA

A publication of the
American Institute of Aeronautics and Astronautics, Inc.
370 L'Enfant Promenade, SW
Washington, DC 20024-2518

JOURNAL OF SPACECRAFT AND ROCKETS
Vol. 32, No. 5, September–October 1995

Integrated Controls–Structures Design Methodology for Flexible Spacecraft

P. G. Maghami,* S. M. Joshi,† and D. B. Price‡
NASA Langley Research Center, Hampton, Virginia 23681

This paper proposes an approach for the design of flexible spacecraft, wherein the structural design and the control system design are performed simultaneously. The integrated design problem is posed as an optimization problem in which both the structural parameters and the control system parameters constitute the design variables, which are used to optimize a common objective function, thereby resulting in an optimal overall design. The approach is demonstrated by application to the integrated design of a geostationary platform, and to a ground-based flexible structure experiment. The numerical results obtained indicate that the integrated design approach generally yields spacecraft designs that are substantially superior to the conventional approach, wherein the structural design and control design are performed sequentially.

Nomenclature

A_c	= compensator state matrix
A_{cl}	= closed-loop system state matrix
B	= control influence matrix
B_c	= compensator input influence matrix
C	= pointing-error influence matrix
d_i	= outer diameter of structural elements in section i
d_{max}	= maximum allowable value for d_i
d_{min}	= minimum allowable value for d_i
E	= steady-state average control power
E_{max}	= maximum allowable steady-state average control power
e	= pointing-error vector
$\mathcal{E}(\ )$	= expected-value operator
G	= compensator output matrix
G_p	= symmetric and nonnegative-definite position gain matrix
G_r	= symmetric and nonnegative-definite rate gain matrix
J	= objective function for design optimization
L_p	= Cholesky factor matrix for the position gain matrix
L_r	= Cholesky factor matrix for the rate gain matrix
M_{act}	= mass of the actuators
M_{max}	= maximum allowable mass of the system
M_{str}	= total mass of the system
P	= positive-definite solution matrix in the Kalman-Yacubovich relations
p_e	= steady-state root-mean-square pointing error
P_e^{max}	= maximum allowable steady-state root-mean-square pointing error
P_x	= state covariance matrix for the system
Q	= arbitrary nonnegative-definite matrix in the Kalman-Yacubovich relations
Tr( )	= trace of ( )
u	= control input vector
z	= plant state vector
x_c	= compensator state vector
y_p	= position output vector
y_r	= rate output vector
α	= constant scalar
$\alpha_{1i}, \alpha_{2i}, \alpha_{3i}, \alpha_{4i}$	= controller design parameters for dynamic dissipative controller
$\|\ \|_\infty$	= infinity norm

Introduction

MANY of space missions under consideration at present, as well as envisioned for the future, will utilize large structures in low Earth and geostationary orbits. Example of such missions include multipayload space science platforms, space antennas, space processing facilities, etc. Such missions typically require large-size, lightweight components such as large solar arrays, antennas, and platforms. However, large size and light weight of such structures results in high flexibility, which makes it more difficult to control them with specified precision in attitude and shape. Therefore, there is a need to develop a methodology for designing space structures that are optimal with respect to both structural design and control design.

The traditional approach to spacecraft design is essentially a sequential one, wherein the structural design is first performed based mainly on the loading, orbital, and thermal considerations. The controller design is next performed to optimize the performance for the fixed structure. However, the performance of the spacecraft so designed is inherently limited. For example, an H-2 or H-infinity controller that is designed to be robust to unmodeled structural dynamics may necessarily have very low gain (and therefore low performance) in order to satisfy the additive uncertainty robustness condition.[1] To obtain higher performance, it would then be necessary to redesign the structure to increase the frequencies of the higher modes and to reduce the effect of the unmodeled dynamics. Another example of necessity of structural redesign is when the transfer-function matrix of the spacecraft has invariant transmission zeros that are within the required controller bandwidth. In that case, the closed-loop transfer function will have deep notches at those frequencies. One way to change the transmission zeros is to move the actuator and sensor locations.[2,3] However, the extent to which the zeros can be moved is limited. For example, when the actuators and sensors are collocated, the frequencies of the zeros can be moved no further than the open-loop structural frequencies. The only way to obtain higher-frequency zeros is to increase the structural mode frequencies, which can only be accomplished by structural redesign. Thus the structural design and the control design problems are substantially coupled, and must be considered concurrently in order to

Received Nov. 12, 1993; revision received Aug. 24, 1994; accepted for publication Sept. 15, 1994.

*Senior Research Engineer, Guidance and Control Branch, Mail Stop 161. Senior Member AIAA.

†Senior Research Scientist, Dynamics and Control Branch, Mail Stop 489. Fellow AIAA.

‡Head, Guidance and Control Branch, Mail Stop 161. Associate Fellow AIAA.

obtain a truly optimal spacecraft design. Let C denote the set of the control design variables (e.g., controller gains), and S the set of the structural design variables (e.g., member sizes). If a structural member thickness is changed, the dynamics will change, which will then change the control law and the required actuator size (and mass). That in turn, will change the structural model. Thus the sets C and S depend on each other, and a methodology for simultaneous optimal control and structure design is highly desirable.

To facilitate analytical treatment, missions involving large space structures can be roughly divided into four classes. Class I missions include flexible spacecraft with no articulated appendages, which require fine attitude pointing and vibration suppression (e.g., large space antennas). Class II missions consist of flexible spacecraft with articulated multiple payloads, where the requirement is to fine-point the spacecraft, and also each individual payload, while suppressing elastic motion. Class III missions include rapid slewing of spacecraft without appendages, and class IV missions include general nonlinear motion of a flexible spacecraft with articulated appendages and robot arms. Class I and II missions represent linear mathematical modeling and control-system design problems (except for actuator and sensor nonlinearities), whereas class III and IV missions represent nonlinear problems.

In this paper, the development of an integrated controls–structures design approach for class I missions is addressed. The integrated design problem is posed in the form of a simultaneous optimization with respect to both the structural and the control design variables. Two controller strategies are considered, namely, the static and dynamic dissipative controllers, which are well known for their stability robustness in the presence of unmodeled dynamics, parametric uncertainties, first-order actuator dynamics, etc. The integrated optimization problem is posed as a single-objective optimization, wherein various measures of performance, such as root-mean-square (rms) pointing errors, transient response, etc., are optimized subject to constraints on the cost defined in terms of the total mass of the spacecraft and/or the required control energy. The integrated design approach is applied to a geostationary platform concept, and also to an experimental test bed.

Controllers for Integrated Design

Control system design for large flexible space structures (LFSSs) is a challenging problem because of their special dynamic characteristics, which include a large number of significant structural modes; low, closely spaced structural mode frequencies; very small inherent damping; and lack of accurate knowledge of the parameters. In order to be practically implementable, the controller must be of a reasonably low order and must also satisfy the performance specifications (i.e., rms pointing error, closed-loop bandwidth, etc.). It must also have robustness to nonparametric uncertainties (i.e., unmodeled structural modes), and to parametric uncertainties (i.e., errors in the knowledge of the design model). Two major categories of controller design methods for LFSS are model-based controllers (MBCs) and dissipative controllers. An MBC generally consists of a state estimator (a Kalman–Bucy filter or an observer) followed by a linear–quadratic regulator. The state estimator utilizes the knowledge of the design model (consisting of the rigid rotational modes and a few structural modes) in its prediction part. Using multivariable frequency-domain design methods, such controllers can be made robust to unmodeled structural dynamics, that is, the spillover effect can be overcome.[1] However, such controllers generally tend to be very sensitive to uncertainties in the design model, in particular, to uncertainty in the structural mode frequencies.[1,4] An analytical explanation of this instability mechanism may be found in Ref. 4. Achieving robustness to real parametric uncertainties is, as yet, an unsolved problem, although considerable research activity is in progress in that area using H-infinity and structured singular-value methods.

In view of the sensitivity problem of MBCs, dissipative controllers, which utilize collocated and compatible actuators and sensors, offer an attractive alternative. Dissipative controllers utilize special passivity-type input–output properties of the plant and offer robust stability in the presence of both nonparametric and parametric uncertainties.[1,5] The simplest controller of this type is the constant-gain dissipative controller. Using collocated and compatible actuators and measurement sensors, the constant-gain dissipative control law is given by

$$u = -G_p y_p - G_r y_r \tag{1}$$

where G_p and G_r are symmetric and nonegative-definite. This control law has been proven to give guaranteed closed-loop stability despite unmodeled elastic modes, parameter errors, certain types of actuator and sensor nonlinearities, and first-order actuator dynamics.[1] The drawback of this controller is that its performance is inherently limited because of its simple mathematical structure.

In order to obtain higher performance while still retaining the highly desirable robust stability, dynamic dissipative compensators can be used. The main characteristic of all dissipative controllers is that they do not rely on the knowledge of the design model to ensure stability, although they utilize it to obtain the best possible performance. A dynamic dissipative controller is given by

$$\dot{x}_c = A_c x_c + B_c y_r \tag{2}$$

$$u = -G x_c - G_r y_r - G_p y_p \tag{3}$$

where A_c is strictly Hurwitz (all its eigenvalues are in the open left half plane), and the positive-realness lemma relations[6] hold:

$$A_c^T P + P A_c = -Q \tag{4}$$

$$G = B_c^T P \tag{5}$$

with $P = P^T > 0$ and $Q = Q^T > 0$.

Equations (2–5) represent a two-level controller, wherein the inner loop consists of a static position-plus-rate feedback and the outer loop consists of a dynamic compensator. This controller assures robust asymptotic stability regardless of unmodeled structural dynamics or parametric uncertainties.[5] In the absence of zero-frequency modes (e.g., for a ground-based experiment), G_p and G_r can be null matrices without destroying the robust asymptotic stability; that is, the inner loop is not required. These results have also been recently extended to systems with zero-frequency modes.[4]

Integrated Design Formulation

The integrated controls–structures design approach was considered for two different systems. The first system is the Earth Pointing System (EPS), which is a multiuser geostationary platform concept. The second system is the Controls–Structures-Interaction (CSI) Evolutionary Model, which is an experimental test bed at NASA Langley Research Center. The two problems are discussed.

Integrated Design of the EPS Model

The EPS concept, shown in Fig. 1, consists of a 10-bay, 30-m-long truss structure with two radial rib antennas (7.5- and 15-m diam) at the ends. All the members (i.e., constituting the truss, the antennas, and the antenna supports) are assumed to be hollow tubes with circular cross section and 1.59-mm thickness. The antennas are assumed to be locked (i.e., fixed with respect to the truss) during normal operation, so that the problem is that of controlling the pointing and vibration of the entire structure. It is assumed that a three-axis control-moment gyro (CMG) and collocated attitude and rate sensors, located at the center of mass of the structure, are used for accomplishing the control.

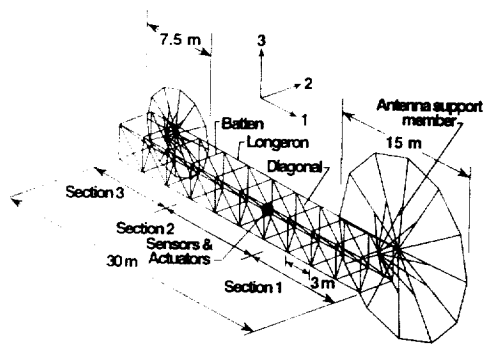

Fig. 1 Schematic of the Earth pointing system.

Table 1 Integrated design of the EPS model

Design	rms pointing, μrad	Structural mass, kg	Actuator mass, kg	Control power, $N^2 \cdot m^2$
Initial	73.6	442.06	150	2.98
Control-optimized	26.9	442.06	150	3.00
Integrated				
without actuator mass	16.94	404.21	150	3.00
with actuator mass	17.01	400.32	298.73	3.00

The approach followed herein is to formulate the integrated design problem as a single-objective optimization problem. The structural design variables used are outer diameters of the truss and antenna support members with the thickness fixed. In particular, the truss was divided into three sections, and the outer diameters of the longerons, battens, and diagonals within each section constitute nine design variables. Two additional structural design variables are the outer diameters of the support members for the two antennas, making a total of 11 structural design variables. A static dissipative control design was chosen for the integrated design with the elements of the Cholesky factorization matrices of the nonnegative-definite position and rate gain matrices chosen as design variables:

$$G_p = L_p L_p^T, \qquad G_r = L_r L_r^T \tag{6}$$

In this design problem, the closed-loop performance measure is the steady-state root-mean-square (rms) pointing error at the large antenna due to white-noise disturbances of unit intensity at the inputs. In order to achieve a realistic design, constraints are placed on the steady-state average control power and the total mass. Additional side constraints are placed on the structural design variables for safety and practicality reasons. Lower bounds are placed on these variables to satisfy structural integrity requirements against buckling and stress failures. On the other hand, upper bounds are placed on these variables to accommodate manufacturing limitations. Thus, the first design problem is as follows:

Minimize the steady-state rms pointing error at the large antenna:

$$J = \min \lim_{t\to\infty} (\mathrm{Tr}\{\mathcal{E}[e(t)e^T(t)]\})^{\frac{1}{2}} \equiv P_e \tag{7}$$

with respect to the tube outer diameters $d_i (i = 1, 2, \ldots, 11)$ and the elements of L_p, L_r, subject to the constraints:

$$E \equiv \lim_{t\to\infty} \mathrm{Tr}\{\mathcal{E}[u(t)u^T(t)]\} \le E_{\max} \tag{8}$$

$$M_{\mathrm{str}} \le M_{\max} \tag{9}$$

$$d_{\min} \le d_i \le d_{\max} \tag{10}$$

Here $e = Cx$ is taken as the 3×1 attitude vector at the large antenna.

The steady-state rms pointing error is computed from the steady-state covariance of the closed-loop state, i.e.,

$$P_e = \left[\mathrm{Tr}\left(C P_x C^T\right)\right]^{\frac{1}{2}} \tag{11}$$

where P_x denotes the steady-state covariance of the state, which is determined from the solution of the following Lyapunov equation[7]:

$$A_{\mathrm{cl}} P_x + P_x A_{\mathrm{cl}}^T = -BB^T \tag{12}$$

The results for this design problem are summarized in Table 1. An initial design based on the nominal structure and a controller, which achieves good rigid-body performance, was first obtained. The nominal structural mass is 442.06 kg, and the actuator mass was assumed constant at 150 kg. For the nominal structure, the first modal frequency was about 0.6 Hz, corresponding to a large antenna-support mode, and the first truss mode was at about 6 Hz. A design model consisting of three rigid-body modes and the first ten flexible modes of the structure was used in the design process. A 0.5% open-loop modal damping was assumed for the flexible modes. The nominal static dissipative control gain matrices were diagonal, with elements chosen to give satisfactory closed-loop frequency and damping for the rigid-body dynamics and to maintain the rms pointing error within the required tolerance.

Table 2 Optimization data for the EPS model

Design Variable	Section	Upper bound, m	Lower bound, m	Initial value, m	Final value, m
1 (longeron)	1	0.15	0.01	0.051	0.107
2 (batten)	1	0.15	0.01	0.051	0.030
3 (diagonal)	1	0.15	0.01	0.051	0.025
4 (longeron)	2	0.15	0.01	0.051	0.066
5 (batten)	2	0.15	0.01	0.051	0.010
6 (diagonal)	2	0.15	0.01	0.051	0.010
7 (longeron)	3	0.15	0.01	0.051	0.066
8 (batten)	3	0.15	0.01	0.051	0.041
9 (diagonal)	3	0.15	0.01	0.051	0.058
10 (support)	Large antenna	0.15	0.01	0.051	0.149
11 (support)	Small antenna	0.15	0.01	0.051	0.010

The integrated design software tool CSI-DESIGN, which is under development at NASA Langley Research Center, was used to perform both the integrated controls–structures designs and control-optimized (or conventional) designs. Employing a four-processor Alliant FX-80 computer, the integrated optimization was performed using the Automated Design Synthesis (ADS) software.[8] An interior penalty function method was used to solve the nonlinear programming problem. Algorithms for minimizing the bandwidth of the banded matrices, as well as expressions for analytical eigenvalue–eigenvector sensitivity, have been incorporated.

With the average control power $E_{\max}$ constrained at 3, the initial design gives an rms pointing error of 73.6 μrad. The conventional design approach was next followed, wherein the control gains (12 elements of the two Cholesky factors L_p and L_r) were optimized for the fixed nominal structure. This control-optimized design yielded an rms pointing error of 26.9 μrad. Next, an integrated design was performed, wherein both the structural and control design variables were allowed to change simultaneously. This resulted in an rms error of 16.9 μrad which represents a 37% reduction from the conventional design. Also, the structural mass was slightly lower than the nominal design. The lower-bound values, upper-bound values, initial values, and optimal values of the structural design variables are summarized in Table 2. The integrated design redistributed the structural mass from the battens and diagonals of the last two sections of the main bus (closest to the small antenna) and small antenna support members to the large antenna support members and the section of the main bus closest to the large antenna, thus increasing the stiffness of these sections. This behavioral trend may be attributed to a tradeoff between structural controllability and observability and its excitability by disturbances. In other words, the stiffness (or flexibility) of the structure is redistributed to establish a balance between the ability of the control system to fine-point the structure efficiently, and the ability of the structure to reject disturbances. The elements of the 3×3 lower-triangular Cholesky factorization matrices L_p and L_r are given in Table 3 for the control-optimized design and the integrated controls–structures design.

In order to evaluate the effect of varying the actuator mass in the integrated design process, the actuator mass was allowed to vary by relating it to the infinity norms of the gain matrices (a worst-case scenario), i.e.,

$$M_{\mathrm{act}} = \alpha |u|_\infty = \alpha(|G_r|_\infty |y_r|_\infty + |G_p|_\infty |y_p|_\infty) \tag{13}$$

For this case the actuator mass increased from 150 to 298.7 kg, while the rms pointing error and the structural mass were essentially unaffected. This is attributed to the fact that the structure is rather stiff and is not affected by small masses. The results obtained clearly show the advantage of integrated design over the conventional approach.

Integrated Design of the Controls–Structures Interaction Evolutionary Model

An important part of the CSI program is the experimental validation of the design methods developed. The CSI Evolutionary Model is a laboratory test bed designed and constructed at NASA Langley

Research Center for experimental validation of the control design methods and the integrated design methodology.[9] The phase-0 evolutionary model, shown in Fig. 2, basically consists of a 62-bay central truss with each bay 10 in. long, two vertical towers, and two horizontal booms. The structure is suspended using two cables as shown. A laser source is mounted at the top of one of the towers, and a reflector with a mirrored surface is mounted on the other tower. The laser beam is reflected by the mirrored surface onto a detector surface 660 in. above the reflector. Eight proportional, bidirectional gas thrusters provide the input actuation, while collocated servo accelerometers provide output measurements. The phase-0 model has six nonstructural modes due to suspension and many significant elastic modes.

To perform the integrated design, the structure was divided into seven sections: three sections in the main bus, and one section each for the two horizontal booms and two vertical towers. Three structural design variables were used in each section, namely, the cross-sectional areas of the longerons, the battens, and the diagonals, making a total of 21 structural design variables. An integrated controls–structures design was obtained by minimizing the steady-state average control power in the presence of a white-noise input disturbance with unit intensity (i.e., standard deviation intensity = 1 lbf), with constraints on the steady-state rms position error at the laser detector (above the structure) and the total mass. That is, the problem solved was as follows:

Minimize

$$E = \lim_{t\to\infty} \mathrm{Tr}\{\mathcal{E}[u(t)u^T(t)]\} \tag{14}$$

Table 3 Elements of Cholesky matrices for the attitude and rate gain matrices of the EPS model

Design Variable	Control-optimized design	Integrated design
$L_p(1,1)$	188.7	254.3
$L_p(2,1)$	7.1	1.2
$L_p(3,1)$	3.9	−1.7
$L_p(2,2)$	179.2	245.0
$L_p(3,2)$	7.4	0.6
$L_p(3,3)$	189.9	255.7
$L_r(1,1)$	212.5	223.3
$L_r(2,1)$	−17.4	−2.9
$L_r(3,1)$	15.3	8.3
$L_r(2,2)$	272.1	327.9
$L_r(3,2)$	−33.0	−1.0
$L_r(3,3)$	293.8	403.3

subject to

$$P_e \equiv \lim_{t\to\infty} \mathrm{Tr}\{\mathcal{E}[e(t)e^T(t)]\}^{\frac{1}{2}} \le P_e^{\max} \tag{15}$$

and a constraint on the total mass

$$M_{\mathrm{str}} \le M_{\max} \tag{16}$$

Here, the pointing-error vector e is taken as the 2×1 vector of the position error at the laser detector. Both static and dynamic dissipative controllers were used in the integrated design of the CSI Evolutionary Model. Velocity signals required for feedback by the dissipative controllers were obtained by processing the accelerometer outputs. The static dissipative controller uses an 8×8 diagonal rate-gain matrix with no position feedback. (Since this system has no zero-frequency eigenvalues, position feedback is not necessary for asymptotic stability.) Thus, in the integrated design with the static dissipative controller, the total number of design variables was 29. The dynamic dissipative controller used in the design was a 32-order controller consisting of eight fourth-order compensators (one for each control channel). The compensator state matrix A_c and input influence matrix B_c were defined as follows:

$$A_c = \begin{bmatrix} A_{c1} & 0 & \cdots & 0 \\ 0 & A_{c2} & \cdots & 0 \\ \vdots & \vdots & \vdots & \vdots \\ 0 & 0 & \cdots & A_{c8} \end{bmatrix} \tag{17}$$

$$B_c = \begin{bmatrix} B_{c1} & 0 & \cdots & 0 \\ 0 & B_{c2} & \cdots & 0 \\ \vdots & \vdots & \vdots & \vdots \\ 0 & 0 & \cdots & B_{c8} \end{bmatrix} \tag{18}$$

where A_{ci} and B_{ci}, $i = 1, 2, \ldots, 8$, are, respectively, 4×4 matrices and 4×1 vectors, defined in a controllable canonical form as

$$A_{ci} = \begin{bmatrix} 0 & 1 & 0 & 0 \\ 0 & 0 & 1 & 0 \\ 0 & 0 & 0 & 1 \\ -\alpha_{4i} & -\alpha_{3i} & -\alpha_{2i} & -\alpha_{1i} \end{bmatrix}, \qquad B_{ci} = \begin{bmatrix} 0 \\ 0 \\ 0 \\ 1 \end{bmatrix} \tag{19}$$

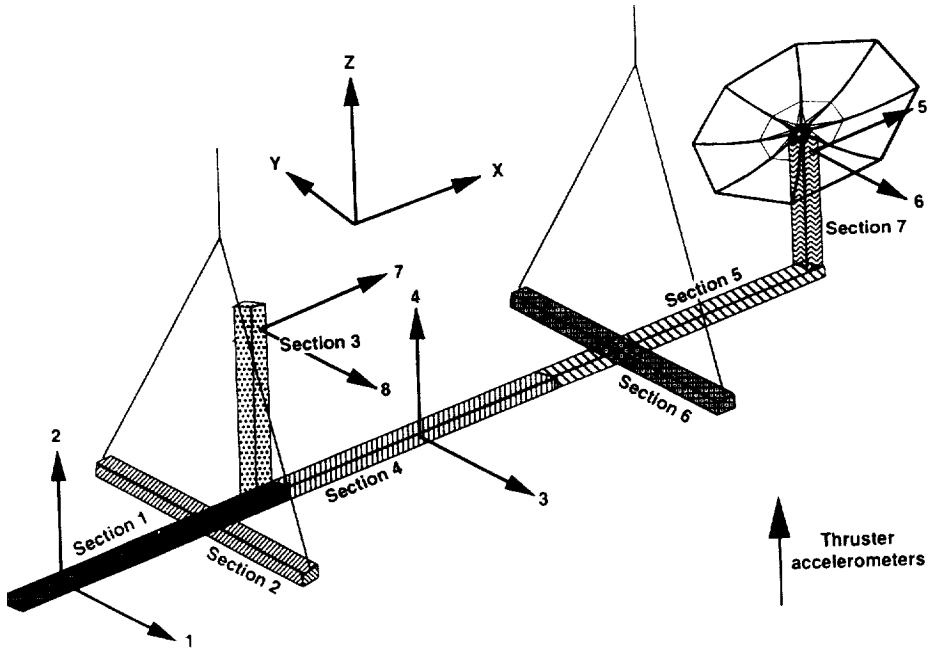

Fig. 2 Schematic of the CSI phase-0 evolutionary model.

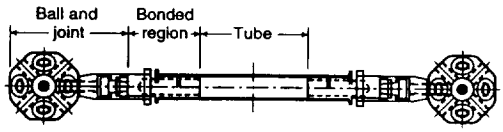

Fig. 3 Typical strut of the CSI evolutionary model.

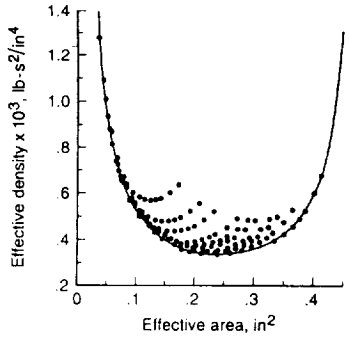

Fig. 4 Strut design curve for battens and longerons.

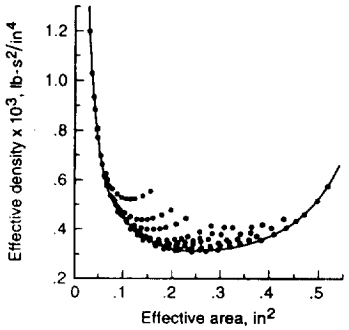

Fig. 5 Strut design curve for diagonals.

Furthermore, the weighting matrix Q in Eq. (4) is assumed to be diagonal, i.e.,

$$Q = \text{Diag}(q_1, q_2, \ldots, q_{32}) \tag{20}$$

Here, the scalar variables $\alpha_{1i}, \alpha_{2i}, \alpha_{3i}, \alpha_{4i}, i = 1, 2, \ldots, 8$, and $q_j, j = 1, 2, \ldots, 32$, were chosen for the control design variables. Thus, the number of control design variables was 64, making the total number of design variables 85. The finite element model of the system has 3216 degrees of freedom; therefore, the bulk of the computational effort is required for the solution of the structural eigenvalue problem of that size. The design model consisted of the first 20 normal modes of the structure, including six suspension modes (modes due to the suspension of the structure) and 14 elastic modes.

In finite element modeling, truss elements are usually modeled as homogeneous beam elements with uniform cross sections. This implies that the mass of the element varies linearly with its cross-sectional area, i.e., the mass density is constant. However, this is not the case for the CSI Evolutionary Model, as shown in Fig. 3. This figure shows a typical strut of the CSI Model, where it is observed that the strut is rather nonuniform and is composed of three separate sections, namely, joint area, bond area, and tube. This nonuniformity of the strut makes the integrated design a bit more complicated, since the effective mass density is not constant but is a function of the effective cross-sectional area. Therefore, one cannot increase or decrease the cross-sectional area of a strut arbitrarily, without considering the nonlinear effects on the structural mass. In order to ensure that the design coming out of the integrated design process is realistic and fabricable, design guides have been developed for longerons and battens (see Fig. 4) and diagonals (see Fig. 5). Each of the points on these design guides represent a fabricable strut with certain tube thickness and diameter. The lowermost points in these figures have been curve-fitted by a rational function of the effective area. These curves are minimum-mass design curves (since they represent design points with the smallest mass densities), which are used in the integrated design process to obtain realizable designs.

Table 4 Integrated design of the CSI evolutionary model

Design	rms displacement, in.	Control power, lb^2
Open loop		
initial structure	38.02	0.00
integrated structure	33.52	0.00
Control-optimized		
S	4.00	7.87
D	4.00	6.63
Integrated		
S	4.00	3.80
D	4.00	3.36

Table 5 Optimization data for the CSI evolutionary model

Design variable	Lower bound, in.	Upper bound, in.	Initial value, in.	Final value, in.
1	0.08	0.38	0.15	0.273
2	0.05	0.38	0.08	0.094
3	0.05	0.48	0.08	0.128
4	0.08	0.38	0.08	0.08
5	0.05	0.38	0.08	0.050
6	0.05	0.48	0.08	0.050
7	0.08	0.38	0.08	0.261
8	0.05	0.38	0.08	0.082
9	0.05	0.48	0.08	0.086
10	0.08	0.38	0.15	0.339
11	0.05	0.38	0.08	0.080
12	0.05	0.48	0.08	0.111
13	0.08	0.38	0.15	0.298
14	0.05	0.38	0.08	0.085
15	0.05	0.48	0.08	0.148
16	0.08	0.38	0.08	0.080
17	0.05	0.38	0.08	0.051
18	0.05	0.48	0.08	0.051
19	0.05	0.38	0.08	0.121
20	0.05	0.38	0.08	0.050
21	0.05	0.48	0.08	0.053

The results of the integrated design is presented in Table 4. Using a constraint on the maximum rms pointing error of 4.0 in. and a constraint on the total mass of 1.92 lb $\cdot$ s^2/in. (nominal mass of the CSI Evolutionary Model), a conventional control-optimized design was performed first (with the structural design fixed at the initial values) using both the static and dynamic dissipative controllers, where the average control power [Eq. (14)] was minimized with respect to the control design variables only. The static dissipative controller gave an average control power of 7.87 lb^2, whereas the dynamic dissipative controller gave a better average control power of 6.63 lb^2.

Next, an integrated design with the static dissipative controller was performed, wherein the average control power E is minimized with respect to both control and structural design variables. The integrated design reduced the average control power by more than 50% to 3.80 lb^2, which demonstrates the clear advantage of integrated design over the traditional sequential design. Using this integrated design as the initial design, another integrated design using the dynamic dissipative controller was performed. This design gave an almost 50% reduction in the average control power from its corresponding control-optimized design. However, the structure did not change much, thus indicating that the structure obtained with the static dissipative controller is also an optimal structure for this dynamic dissipative controller. The results clearly show that an integrated design can yield a substantial improvement in the overall design.

The initial and final values of the structural design variables, along with the corresponding lower bound and upper bound values are presented in Table 5. Keeping in mind that the tube cross-sectional areas of the nominal CSI Evolutionary Model structure are 0.134 in.^{2} for the longerons and battens and 0.124 in.^{2} for the diagonal, it is observed from Table 4 that all three sections of the main bus (particularly the middle section) and the laser tower are considerably stiffened, while the horizontal booms and the reflector tower became more flexible, partly to satisfy the mass constraint. Generally, in those sections that showed an increase in stiffness,

Table 6 Diagonal elements of rate gain matrices for the CSI evolutionary model (static dissipative controller)

Design variable	Control-optimized design	Integrated design
$G_r(1, 1)$	0.245	0.283
$G_r(2, 2)$	0.627	0.289
$G_r(3, 3)$	0.425	0.210
$G_r(4, 4)$	1.566	0.220
$G_r(5, 5)$	0.743	0.198
$G_r(6, 6)$	0.355	0.208
$G_r(7, 7)$	0.449	0.281
$G_r(8, 8)$	0.268	0.476

Table 7 Control design variables for the CSI evolutionary model (dynamic dissipative controller)

Design variable	Control-optimized design	Integrated design	Design variable	Control-optimized design	Integrated design
$A_c(4, 1)$	27.84	85.33	$A_c(20, 17)$	27.47	79.81
$A_c(4, 2)$	153.47	305.30	$A_c(20, 18)$	108.79	242.39
$A_c(4, 3)$	184.48	260.52	$A_c(20, 19)$	136.0	208.00
$A_c(4, 4)$	50.43	76.47	$A_c(20, 20)$	40.44	86.44
$A_c(8, 5)$	26.49	86.40	$A_c(24, 21)$	28.08	78.46
$A_c(8, 6)$	165.54	355.55	$A_c(24, 22)$	126.61	264.51
$A_c(8, 7)$	169.55	210.11	$A_c(24, 23)$	173.12	228.82
$A_c(8, 8)$	103.21	88.65	$A_c(24, 24)$	44.41	79.66
$A_c(12, 9)$	15.70	73.17	$A_c(28, 25)$	37.61	78.75
$A_c(12, 10)$	168.42	324.34	$A_c(28, 26)$	172.98	263.11
$A_c(12, 11)$	198.67	289.22	$A_c(28, 27)$	155.55	221.37
$A_c(12, 12)$	92.14	87.33	$A_c(28, 28)$	103.41	89.15
$A_c(16, 13)$	18.99	71.88	$A_c(32, 29)$	26.00	111.66
$A_c(16, 14)$	157.75	320.62	$A_c(32, 30)$	109.89	317.25
$A_c(16, 15)$	51.20	242.72	$A_c(32, 31)$	271.28	411.62
$A_c(16, 16)$	102.61	89.53	$A_c(32, 32)$	55.63	82.87

Table 8 Control design variables for the CSI evolutionary model (dynamic dissipative controller)

Design variable	Control-optimized design	Integrated design	Design variable	Control-optimized design	Integrated design
$Q(1, 1)$	3959.7	4395.2	$Q(17, 17)$	3739.4	3587.9
$Q(2, 2)$	8225.0	12008.9	$Q(18, 18)$	7461.6	10329.9
$Q(3, 3)$	4879.7	11986.5	$Q(19, 19)$	4469.6	10280.3
$Q(4, 4)$	518.1	3919.9	$Q(20, 20)$	637.6	3626.6
$Q(5, 5)$	3033.9	4350.1	$Q(21, 21)$	3889.8	3600.1
$Q(6, 6)$	6749.3	12481.5	$Q(22, 22)$	7792.7	9997.3
$Q(7, 7)$	3584.0	12034.5	$Q(23, 23)$	4585.0	10014.4
$Q(8, 8)$	565.2	4351.7	$Q(24, 24)$	549.2	3558.6
$Q(9, 9)$	3103.4	3315.9	$Q(25, 25)$	3150.6	4303.9
$Q(10, 10)$	6588.5	9453.8	$Q(26, 26)$	7345.8	12646.7
$Q(11, 11)$	3915.9	9414.6	$Q(27, 27)$	3670.0	12690.7
$Q(12, 12)$	276.6	3447.3	$Q(28, 28)$	746.4	4334.0
$Q(13, 13)$	3237.9	3397.7	$Q(29, 29)$	3348.2	7749.0
$Q(14, 14)$	7346.2	9804.8	$Q(30, 30)$	6710.7	20403.1
$Q(15, 15)$	4533.8	9698.0	$Q(31, 31)$	2469.4	22056.7
$Q(16, 16)$	588.5	3307.7	$Q(32, 32)$	412.2	7474.9

the longerons increased in size more than the diagonals and the battens, since they are most effective in changing the stiffness of a section. The trends in Table 5 may be attributed to a tradeoff between structural controllability, observability, and excitability. The areas near the disturbance sources (actuator locations) were stiffened in order to reduce the sensitivity of the structure to external disturbances at those locations, while ensuring that no appreciable loss of controllability and/or observability occurred. The diagonal elements of the rate gain matrix for the static dissipative controller are given in Table 6 for the control-optimized design and the integrated controls–structures design. It is observed that the elements of the rate gain matrix for the integrated design are generally smaller than those for the control-optimized design except for channels 1 and 8. The elements of the compensator state matrix A_c are given in Table 7 for the control-optimized design and the integrated controls–structures design. Also, the elements of the weighting matrix Q are presented in Table 8 for both designs.

The results obtained for both the static and dynamic dissipative controllers clearly show that integrated controls–structures design methodology can yield a substantially superior overall design to the conventional sequential design scenario.

Concluding Remarks

An optimization-based approach has been developed for performing integrated controls–structures design of a class of flexible spacecraft. The approach formulates the problem as a constrained optimization problem, wherein the design variables consist of both control and structural design variables. The approach uses static and dynamic dissipative control laws, which provide robust stability in the presence of parametric and nonparametric uncertainties. The approach was demonstrated by application to integrated designs of a geostationary platform concept, as well as a ground experiment test bed. The numerical results obtained indicate that the integrated design approach can yield substantially superior spacecraft designs to those from the traditional sequential design approach. Furthermore, the automated nature of the integrated design approach can accommodate a wide variety of design specifications and requirements. A practical software tool (CSI-DESIGN) is being developed for performing integrated designs.

Acknowledgment

The authors would like to thank Kenny Elliott of NASA Langley Research Center for providing the strut design guides (Figs. 4 and 5).

References

[1]Joshi, S. M., *Control of Large Flexible Space Structures*, edited by M. Thoma and A. Wyner, Vol. 131, Lecture Notes in Control and Information Sciences, Springer–Verlag, Berlin, 1989.

[2]Maghami, P. G., and Joshi, S. M., "Sensor/Actuator Placement for Flexible Space Structures," *IEEE Transactions on Aerospace and Electronic Systems*, Vol. 29, No. 2, 1993, pp. 345–351; see also *Proceedings of the 1990 American Control Conference*, Vol. 2, 1990, pp. 1941–1948.

[3]Williams, T., "Computing the Transmission Zeros of Large Space Structures, " *IEEE Transactions on Automatic Control*, Vol. 34, No. 1, 1989, pp. 92–94.

[4]Joshi, S. M., Maghami, P. G., and Kelkar, A. T., "Dynamic Dissipative Compensator Design for Flexible Spacecraft Structures," AIAA Paper 91-2650, Aug. 1991.

[5]Joshi, S. M., and Maghami, P. G., "Dissipative Compensators for Flexible Spacecraft Control " *IEEE Transactions on Aerospace and Electronic Systems*, Vol. 28, No. 3, 1992, pp. 768–774; see also *Proceedings of the 1990 American Control Conference*, Vol. 2, 1990, pp. 1955–1961.

[6]Anderson, B. D. O., "A System Theory Criterion for Positive-Real Matrices," *SIAM Journal of Control*, Vol. 5, No. 2, 1967, pp. 171–182.

[7]Stengel, R. F., *Stochastic Optimal Control: Theory and Applications*, Wiley, New York, 1986.

[8]Vanderplaats, G. N., "ADS—A Fortran Program for Automated Design Synthesis—Version 1.10," NASA Contractor Report 177985, Sept. 1985.

[9]Belvin, W. K., Elliott, K. B., Horta, L. G., Bailey, J. P., Bruner, A. M., Sulla, J. L., Won, J., and Ugoletti, R. M., "Langley's CSI Evolutionary Model: Phase 0," NASA TM-104165, Nov. 1991.

E. A. Thornton
Associate Editor